



Sound transmission loss for double panels using the Wave Finite Element Method

G. P. Zanoni¹, A. L. Serpa¹

¹*School of Mechanical Engineering, University of Campinas (UNICAMP)
Mendeleyev St., 200, Campinas, 13083-860, São Paulo, Brazil
giovannapzanoni@gmail.com, alserpa@unicamp.com*

Abstract. Double panels are a usual solution for noise control. In this study, the sound transmission loss (STL) of an infinite double panel with an air cavity and two solid layers was analyzed. The STL was calculated from a dynamic stiffness matrix of the system, where the air layer was modeled analytically, and the solid layers were modeled using the Wave Finite Element (WFE) method, where only one small segment of the structure is modeled using conventional Finite Element Method (FEM), reducing the computational cost. The influence of the thickness of the cavity and the specific masses per area of the solid layers in the STL were analyzed. Also, an optimization procedure to maximize STL in different octave bands was performed. The results demonstrated that the WFE method is suitable for STL calculation; that a higher STL is obtained for a wider air cavity and higher specific mass (below coincidence frequency), and the optimization procedure led to different optimal parameters depending on frequency because of various physical phenomena presented at a double panel.

Keywords: Sound transmission loss, Wave Finite Element method, Double panel.

1 Introduction

Acoustic panels are used in various applications, and they can be simple, containing a unique layer of one material, or they can be multi-layered panels. Barron [1] and Raichel [2] cite examples of acoustic multi-layered partitions: double glass windows, sandwich panels used in sound enclosures or noise barriers for machinery noise and drywall panels used in civil construction.

A usual configuration is a double panel separated by an air gap. The air space dynamically couple the two panels, and this has an effect on STL. Fahy and Gardonio [3] explains that the double panel has a minimum of STL at its mass-air-mass resonance, which depends on the thickness of the air cavity (d) and the mass per unit area of the solid layers. Below the mass-air-mass resonance, the double panel behaves as one panel, and just after the mass-air-mass resonance, the inertia dominates the system. For higher frequencies, the behavior of the STL curve is dictated by the resonances and anti-resonances of the air cavity.

In Fahy and Gardonio [3], the coincidence frequency for oblique sound incidence is also studied. It occurs when the parallel component of the wavenumber of the incident wave is equal to the bending wavenumber in a partition. In this frequency, the STL is minimized.

Analytical models are available for the prediction of STL of multi-layer panels, especially when the materials used are isotropic and with simple geometry, such as the models of Mulholland et al. [4], Fahy and Gardonio [3] and Barron [1]. Also, the transfer function method can be used for this calculation. However, for more complicated geometry and orthotropic materials, the use of the transfer function method becomes impractical because of lengthy expressions, as discussed in Yang et al. [5]. An alternative is the use of Finite Element Analysis, which is also a well-established methodology. In the case of structures that can be divided into periodic cells that are repeated in one or two directions, the Wave Finite Element (WFE) method can be used to reduce the computational cost.

In the WFE method, only one periodic cell is discretized using a Finite Element mesh, and periodic conditions are applied to describe wave propagation in the entire structure, using the information of the Dynamic Stiffness of the periodic cell, obtained by mass and stiffness matrices. The dispersion relation can be found for one dimensional propagation in Mace et al. [6] and for two dimensional wave propagation in Mace and Manconi [7]. More recently,

the prediction of sound transmission loss using WFE was developed by Yang et al. [5] using an analysis of fluid-structure interaction.

In this study, the WFE method was used to perform the STL calculations for a panel composed of two solid layers separated by an air space. The STL behavior was studied for different thickness values and for different values of mass per unit area of the solid layers. An optimization procedure of the air thickness and the mass per unit area of the solid layers was performed in order to maximize STL at different octave bands.

2 Calculation of sound transmission loss

The STL for a double panel separated by an air cavity was calculated using the WFE method considering 2D wave propagation as in Mace and Manconi [7] and the STL calculation as in Yang et al. [5]. The proposed panel is composed of two layers of steel and an air cavity, and the layers are assumed to be infinite (Fig. 1).

In Yang et al. [5] the air cavity layer has been modeled analytically, so the spectral dynamic stiffness matrix (\mathbf{D}_{air}), which relates the acoustic pressures and the displacements at the boundaries of the layers, is:

$$\mathbf{D}_{\text{air}} = \frac{\rho_0 \omega^2}{\sin(k_{z0}d)} \begin{bmatrix} -\cos(k_{z0}d) & 1 \\ -1 & \cos(k_{z0}d) \end{bmatrix}, \quad (1)$$



Figure 1. Acoustic pressures (p) at different layers of an infinite double panel; A, B, or C superscripts indicate the corresponding layer, and 1 and 2 subscripts indicate acoustic pressure at the upper surface of the layer and bottom surface of the layer, respectively.

where ρ_0 is the air density, k_{z0} is the z component of the wavenumber in air and ω is the angular frequency.

An infinite partition can be described as a periodical material so in the WFE method, only a small substructure of it is discretized using FEM. In this study, the substructure of each solid layer was discretized using isoparametric hexahedron finite elements, a type of solid finite element. The equations for mass and stiffness matrices of this element are described in Know and Bang [8] and Petyt [9]. Six finite elements were used with $l_z = h/6$ and $l_x = l_y = l_z$, where h is the thickness of the solid layer and l_x , l_y , l_z are the lengths in x , y , z directions of one finite element (Fig 2a). Through the thickness of the solid layers, the nodes were described as hypernodes (a vector containing all degrees of freedom of these nodes). For example, hypernode 1 (\mathbf{q}_1) (Fig. 2b) contains the degrees of freedom of nodes 1,5,9,13,17,21,25 (Fig. 2a).

Based on Bloch-Floquet theorem, propagation constants can be used when modeling periodical materials as described in Mace and Manconi [7] and Yang et al. [5]. The propagation constants are: $\lambda_x = e^{-i\mu_x}$ and $\lambda_y = e^{-i\mu_y}$, where $\mu_x = k_x L_x$, $\mu_y = k_y L_y$, and k_x and k_y are the wavenumbers in x and y direction and L_x and L_y are the length of one periodic cell in x and y directions, respectively. Considering the geometrical disposition of the hypernodes (Fig. 2b), the propagation constants were applied to describe the hypernodes $\mathbf{q} = [\mathbf{q}_1, \mathbf{q}_2, \mathbf{q}_3, \mathbf{q}_4]$ as a function of \mathbf{q}_1 as:

$$\mathbf{q} = \left\{ \mathbf{I} \quad \mathbf{I}\lambda_x \quad \mathbf{I}\lambda_x\lambda_y \quad \mathbf{I}\lambda_y \right\}^T \mathbf{q}_1 = \mathbf{\Lambda}_R \mathbf{q}_1, \quad (2)$$

The acoustics forces that act on the solid layers because of the incident, reflected, and transmitted waves can be lumped at the hypernodes. The sum of the forces on \mathbf{q}_1 can be described using the propagation constants:

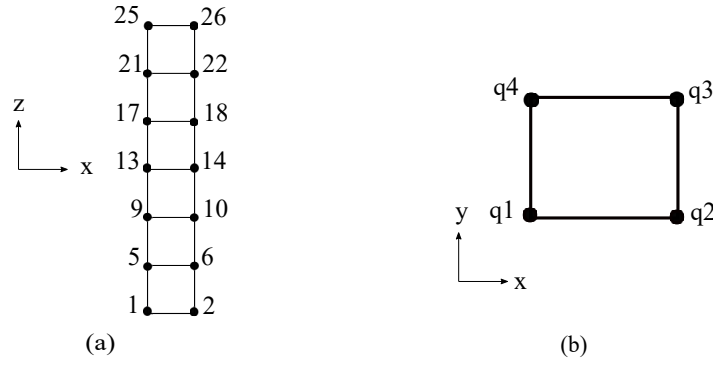


Figure 2. Substructure of one solid layer: (a) nodes numeration of the solid elements through thickness (front view) and (b) hypernodes numeration (top view); different scales were used.

$$\left\{ \mathbf{I} \quad \mathbf{I}\lambda_x^{-1} \quad \mathbf{I}\lambda_x^{-1}\lambda_y^{-1} \quad \mathbf{I}\lambda_y^{-1} \right\} \mathbf{f} = \Lambda_L \mathbf{f}, \quad (3)$$

where $\mathbf{f} = [\mathbf{f}_1, \mathbf{f}_2, \mathbf{f}_3, \mathbf{f}_4]^T$ is the vector of forces at the hypernodes.

Substituting eq.(2) in the dynamic motion equation ($\mathbf{D}\mathbf{q} = \mathbf{f}$) and pre-multiplying the resulting expression by Λ_L of eq.(3) it is possible to write:

$$\Lambda_L \mathbf{D} \Lambda_R \mathbf{q}_1 = \Lambda_L \mathbf{f}, \quad (4)$$

where $\mathbf{D}_r = \Lambda_L \mathbf{D} \Lambda_R$ is the reduced dynamic stiffness matrix. The components of vector \mathbf{f} can be calculated using the expressions presented in Yang et al. [5].

Now, a matrix called $\mathbf{D}_{\text{solid}}$ (size of 2×2) is created by condensing the matrix \mathbf{D}_r leaving only the degrees of freedom of the displacements in z direction of the upper and lower surfaces of the solid layer. $\mathbf{D}_{\text{solid}}$ is calculated for each solid layer (A and C), following the previous steps (the layers can be different and consequently have different dynamic stiffness matrices). These expressions and eq. 1 are used to write the global stiffness matrix of the double panel system (\mathbf{D}_{sys}):

$$\mathbf{D}_{\text{sys}} = \begin{bmatrix} \mathbf{D}_{\text{solid}}^A & \mathbf{0} & \mathbf{0} \\ \mathbf{0} & \mathbf{D}_{\text{air}} & \mathbf{0} \\ \mathbf{0} & \mathbf{0} & \mathbf{D}_{\text{solid}}^C \end{bmatrix}. \quad (5)$$

The next step was to condense the internal surface displacements of \mathbf{D}_{sys} , to write a new matrix that relates the displacements in z direction (u_z) and the acoustic pressures at the upper boundary of layer A (p_1^A) and the bottom boundary of layer C (p_2^C) (Fig. 1). The variables were organized as in Yang et al. [5], and the dynamic condensation was applied, leading to a 2×2 matrix named \mathbf{D}_{sr} :

$$\mathbf{D}_{\text{sr}} \begin{bmatrix} u_z^A \\ u_z^C \end{bmatrix} = \begin{bmatrix} p_1^A \\ p_2^C \end{bmatrix}. \quad (6)$$

Considering the dynamic stiffness of the air surrounding the double plate, it is known that:

$$p_1^A = 2p_{\text{inc}} - i\rho_0\omega^2 u_z^A / k_{z0}, \quad (7)$$

where p_{inc} is the complex amplitude of the incident wave, and:

$$p_2^C = -i\rho_0\omega^2 u_z^A / k_{z0}. \quad (8)$$

Substituting eq. (7) and eq. (8) in eq. (6), one can find the equation:

$$\mathbf{D}_{sr} + \mathbf{D}_{\infty} \begin{bmatrix} u_z^A \\ u_z^C \end{bmatrix} = \begin{bmatrix} 2p_{inc} \\ 0 \end{bmatrix}, \text{ with } \mathbf{D}_{\infty} = \begin{bmatrix} -i\rho_0\omega^2/k_z & 0 \\ 0 & -i\rho_0\omega^2/k_z \end{bmatrix}. \quad (9)$$

Equation (9) is solved for the vector of displacements. Using these displacements, the acoustic pressures on the external surfaces of the double panel can be found using eq. (7) and eq. (8).

Finally, the sound transmission coefficient can be given by:

$$\tau(\omega) = \frac{Re(|p_2^C|^2)}{|p_{inc}|^2}, \quad (10)$$

The sound transmission loss is obtained by the expression $STL = -10 \log_{10}(\tau)$.

3 Results and Discussion

Using the calculation procedure presented in Section 2, the STL was calculated for different configurations of different air thickness (d) and different masses per unit area of the solid layers (m_A and m_C) for an oblique incidence angle of $\theta = 60^\circ$. The material of the solid layers were steel, an usual material for noise barriers and enclosures, with density of $\rho = 7800 \text{ kg/m}^3$, Poisson coefficient of $\nu = 0.28$, Young modulus of $E = 20 \text{ GPa}$ and loss factor of $\eta = 0.03$ (Yang, 2018). A complex Young modulus, $E = E(1 + i\eta)$, was considered to account for structural damping. The analyzed frequency range was from 100 to 20000 Hz .

3.1 Influence of the thickness of the air cavity and the mass per unit area of the solid layers

First, the influence of the variation with different air thick thickness (d) was investigated (Fig. 3) for d of values 10, 15, 20, 25, 30 mm using a constant thickness of 2 mm of the two solid layers. For each curve in the graph, the first valley refers to the mass-air-mass resonance, which is shifted to higher frequencies as the separation of the solid layers increase; the second valley, around 8000 Hz , which did not vary in frequency for the five cases analyzed, corresponds to the coincidence frequency because this phenomenon is directly linked to the angle of incidence and the characteristics of the solid layers, which were constant in this analysis. The other valleys in the curves referred to the air cavity resonances. These resonances are related to the formation of stationary waves in the air cavity, so its thickness influences the frequency of the stationary waves. For a better STL performance between the mass-air-mass resonance and the coincidence frequency, it was necessary to increase d , however for a better STL performance above coincidence, it is essential to decrease d , so the lowest resonance frequency of the cavity is shifted to a higher frequency.

Second, the influence of using different specific masses per area (m_A and m_C) and using the same m_A and m_C in the two solid layers was analyzed using different configurations described in Table 1. In order to vary m_A and m_C , combinations of different thicknesses were proposed because the material is the same in both layers. The separation of the plate was $d = 20 \text{ mm}$.

When analyzing Fig. 4, one can see that all of the curves had a STL valley around 17000 Hz , due to the air cavity resonance for $d = 20 \text{ mm}$; the same valley was found in Fig. 3 for this thickness. For cases 2, 3, and 5, where the thicknesses of the layers are different, two coincidence dips occur. This indicate a behavior of the solid layers as plates with different thickness. The wavenumber in a plate is related to bending stiffness and consequently related to the thickness of the plate. In cases 1, 2, and 3, the coincidence frequency around 1620 Hz was related to the layer with 1 mm thickness and was close to the air cavity resonance, so their regions of decreasing STL merged. In general, the configuration with greater total mass, case 6, had the higher STL, however, this is not valid for the coincidence region. Also, case 6 led to the greatest mass-air-mass resonance, demonstrating that the increase of total mass increases the mass-air-mass resonance, as expected from Fahy and Gardonio [3].

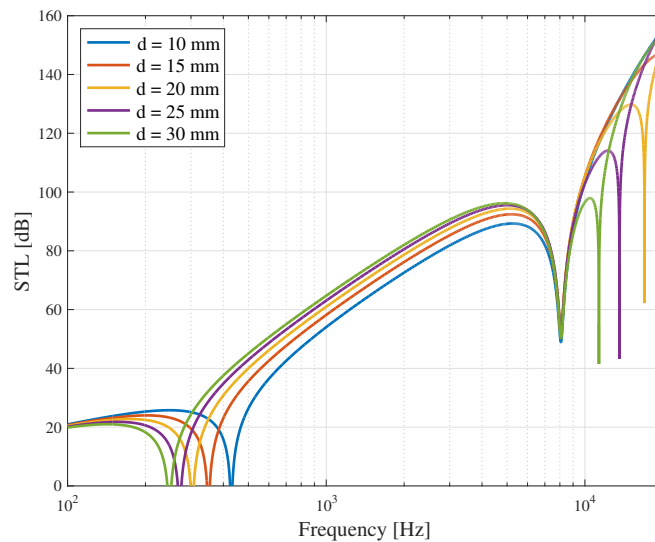


Figure 3. Variation of sound transmission loss (STL), for different air cavity thickness (d).

Table 1. Cases of double panel using different thickness for the layers

| Case | Thickness of layer A (h_A) | Thickness of layer C (h_C) |
|--------|--------------------------------|--------------------------------|
| Case 1 | 1 mm | 1 mm |
| Case 2 | 1 mm | 1.5 mm |
| Case 3 | 1 mm | 2 mm |
| Case 4 | 1.5 mm | 1.5 mm |
| Case 5 | 1.5 mm | 2 mm |
| Case 6 | 2 mm | 2 mm |

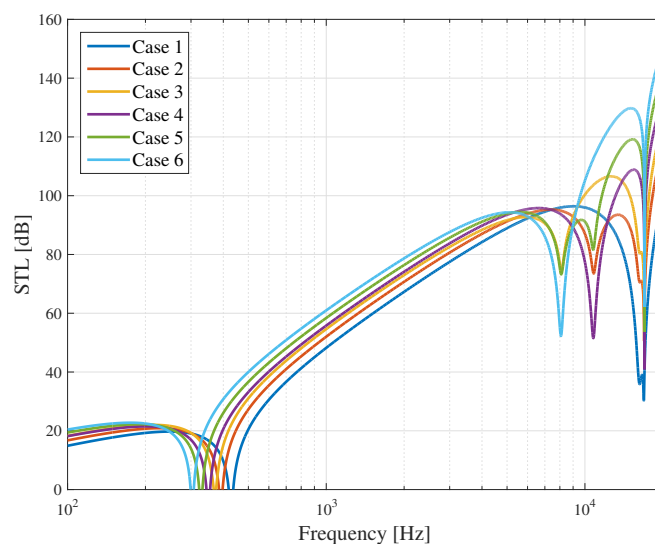


Figure 4. Variation of sound transmission loss (STL), for different thickness of the solid layers (h_A and h_C), cases described in Table 1.

3.2 Optimization

In many cases, for applications of machinery noise control, the octave band of lower frequencies contains the most significant sound levels. A double panel can be used as a noise barrier in this case. In practical applications, the measurement of machinery noise sound is performed using octave bands, so an optimization procedure was

implemented to maximize STL in the desired octave band.

To maximize STL is necessary to minimize the sound transmission coefficient (τ). Optimal values of the thickness of the air layer (d) and the thickness of the solid layers (h_A, h_C) need to be found for this optimization. An algorithm of quadratic sequential programming was used to perform this multivariable constrained minimization, and the optimization problem can be described as:

$$\text{minimize } \tau(h_A, h_C, d), \text{ subjected to : } \begin{cases} 1 \text{ mm} \leq h_A \leq 2 \text{ mm}; \\ 1 \text{ mm} \leq h_C \leq 2 \text{ mm}; \\ 10 \text{ mm} \leq d \leq 30 \text{ mm}. \end{cases}$$

An usual noise source in industrial facilities is fan noise, which is directly related to rotation speed and the number of blades in the fan. Because of operational conditions, fan noise is predominant at the octave bands of 125, 250 and 500 Hz. Typical sound levels for fans can be found in Raichel [2].

The optimization procedure was applied to minimize τ at the octave bands of 250 and 500 Hz, separately. For the octave band of 250 Hz, the optimized parameters are: $X_{opt} = [2, 2, 10]$ mm. The STL value was 25 dB at the 250 Hz octave band (Fig. 5); the values of STL for each octave band are indicated as red stars. The reduced value of d in X_{opt} shifted the mass-air-mass resonance to a higher frequency, enabling to maximize STL at this octave band. This effect can be noted at the STL curve with narrow frequency band (Fig. 5).

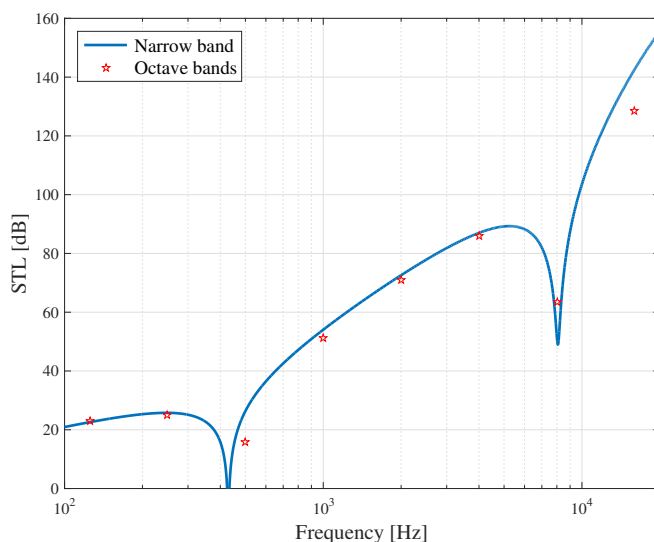


Figure 5. Sound transmission loss (STL) for optimized parameters $h_A = 2$ mm, $h_C = 2$ mm and $d = 10$ mm, to maximize STL for the octave band of 250 Hz.

For the octave band of 500 Hz, the optimized parameters are: $X_{opt} = [2, 2, 30]$ mm. The STL values was 42 dB at the 500 Hz octave band (Fig. 6). As analyzed in the Subsection 3.1, in the region above the mass-air-mass resonance and below the coincidence frequency, the maximum performance is obtained for greater values of d and h_A, h_C .

However, the behavior of the STL curves for double panels is complicated, especially at the coincidence frequency and above it, around the cavity's resonances. In Figs. 5 and 6 the coincidence frequency is around 8000 Hz and in this region STL decreases. If it was desired to increase STL in this frequency region, the optimization problem applied to this octave band led to $X_{opt} = [1, 1, 19.5]$ mm with the STL = 95 dB in this octave band. Note that in this case, the system's total mass is less than in the optimization at the octave bands of 250 and 500 Hz.

Besides the influence of the parameters was analyzed in Section 3.1, the optimization procedure demonstrated to be an efficient method. For low frequencies, especially, where the width of the octave band is narrow, the optimum parameters are found rapidly compared to a manual adjustment of the parameters.

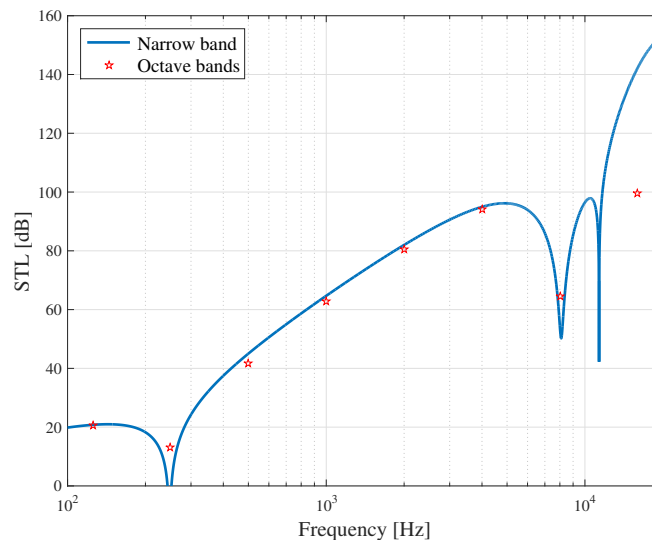


Figure 6. Sound transmission loss (STL) for optimized parameters $h_A = 2 \text{ mm}$, $h_C = 2 \text{ mm}$ and $d = 30 \text{ mm}$, to maximize STL for the octave band of 500 Hz.

4 Conclusions

The sound transmission loss calculation using the Wave Finite Element method successfully predicted the sound transmission loss of the double panel, predicting the phenomena of the mass-air-mass resonance, the coincidence frequency, and the resonance of the cavities with the use of a few finite elements. To obtain a higher mass-air-mass resonance, it is necessary to decrease the thickness of the air layer and to increase the total mass of the solid layers. In general, to enhance STL, a wider air thickness and a greater total mass is needed; however, this is not valid for higher frequencies due to coincidence effects and the air cavity resonances. The optimization procedure can help to find the best parameters of the plate depending on what frequency range one needs to increase the sound transmission loss. Future works will include the use of the Wave Finite Element method to study the sound transmission loss of more complex structures.

Acknowledgements. The authors thank Conselho Nacional de Desenvolvimento Científico e Tecnológico (CNPq) for the financial support.

Authorship statement. The authors hereby confirm that they are the sole liable persons responsible for the authorship of this work, and that all material that has been herein included as part of the present paper is either the property (and authorship) of the authors, or has the permission of the owners to be included here.

References

- [1] R. F. Barron. *Industrial noise control and acoustics*. Marcel Dekker, first edition, 2001.
- [2] D. R. Raichel. *The science and applications of acoustics*. Springer, second edition, 2006.
- [3] F. Fahy and P. Gardonio. *Sound and structural vibration: radiation, transmission and response*. Academic Press, second edition, 2007.
- [4] K. A. Mulholland, H. D. Parbrook, and A. Cummings. The transmission loss of double panels. *Journal of Sound and Vibration*, vol. 6, n. 3, pp. 324–334, 1967.
- [5] Y. Yang, B. R. Mace, and M. J. Kingan. Wave and finite element method for predicting sound transmission through finite multi-layered structures with fluid layers. *Computers and Structures*, vol. 204, pp. 20–30, 2018.
- [6] B. Mace, D. Duhamel, M. Brennan, and L. Hinke. Finite element prediction of wave motion in structural waveguides. *The Journal of the Acoustical Society of America*, vol. 117, n. 5, pp. 2835–2843, 2005.
- [7] B. R. Mace and E. Manconi. Modelling wave propagation in two-dimensional structures using finite element analysis. *Journal of Sound and Vibration*, vol. 318, n. 4-5, pp. 884–902, 2008.
- [8] Y. W. Know and H. Bang. *The finite element method using MATLAB*. CRC Press, first edition, 1997.
- [9] M. Petyt. *Introduction to finite element vibration analysis*. Cambridge University Press, second edition, 2010.